Supplement of Atmos. Chem. Phys., 25, 7991–8028, 2025
https://doi.org/10.5194/acp-25-7991-2025-supplement

Supplement of

Tropospheric ozone trends and attributions over East and Southeast Asia in 1995–2019: an integrated assessment using statistical methods, machine learning models, and multiple chemical transport models

Xiao Lu et al.

Correspondence to: Xiao Lu (luxiao25@mail.sysu.edu.cn)

Table S1. Summary of meteorological variables being used in the multiple linear regression (MLR), the ridge regression (RR), and the random forest regression (RFR) models

Names and units of variables	ERA5 variables	MERRA2 variables	Average period
temperature at 2 m (K)	t2m	T2M	06:00 to 18:00
Solar Radiation	ssrd	SWGDN	06:00 to 18:00
mean sea level pressure (Pa)	msl	SLP	06:00 to 18:00
relative humidity (%)	R	RH	06:00 to 18:00
boundary layer height (m)	blh	PBLH	06:00 to 18:00
zonal wind at 10m (m s^{-1})	u10	U10M	06:00 to 18:00
meridional wind at 10m (m s^{-1})	v10	V10M	06:00 to 18:00
total precipitation (mm)	tp	PRECTOT	06:00 to 18:00[a]
zonal wind at 850hPa (m s^{-1})	u	U	06:00 to 18:00
meridional wind at 850hPa (m s^{-1})	v	V	06:00 to 18:00
vertical velocity at 850hPa (Pa s^{-1})	w	OMEGA	06:00 to 18:00

[a] Total amount in the period

Table S2. Configuration of physical parameterization schemes for the WRF model

Term	**Option**
Microphysics scheme	Purdue Lin scheme
Longwave radiation scheme	RRTM scheme
Shortwave radiation scheme	Goddard shortwave
Surface-layer scheme	Revised MM5 Monin-Obukhov scheme
Land-surface scheme	Unified Noah Land Surface Model
Boundary-layer scheme	Yonsei University scheme
Cumulus scheme	Kain-Fritsch scheme

Table S3. Mean and standard deviations in R^2 in the four city-clusters by different models.

		MLR	RR	RFR
NCP	ERA5	0.38 ± 0.07	0.39 ± 0.07	0.43 ± 0.08
	MERRA-2	0.35 ± 0.05	0.35 ± 0.05	0.38 ± 0.07
YRD	ERA5	0.42 ± 0.08	0.43 ± 0.08	0.55 ± 0.09
	MERRA-2	0.34 ± 0.08	0.36 ± 0.08	0.47 ± 0.09
PRD	ERA5	0.52 ± 0.03	0.54 ± 0.04	0.64 ± 0.05
	MERRA-2	0.50 ± 0.06	0.50 ± 0.06	0.60 ± 0.06
SCB	ERA5	0.24 ± 0.18	0.26 ± 0.18	0.25 ± 0.16
	MERRA-2	0.44 ± 0.03	0.44 ± 0.04	0.47 ± 0.05

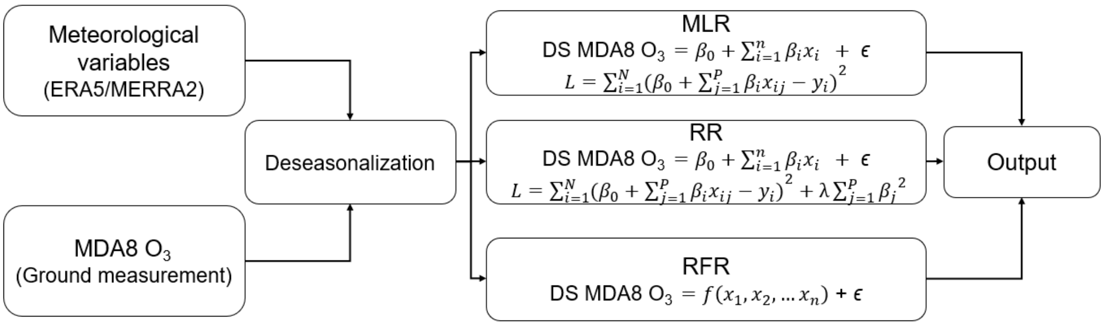

Figure S1. Overview of the statistical and machine learning models used in this study to attribute surface ozone trends.

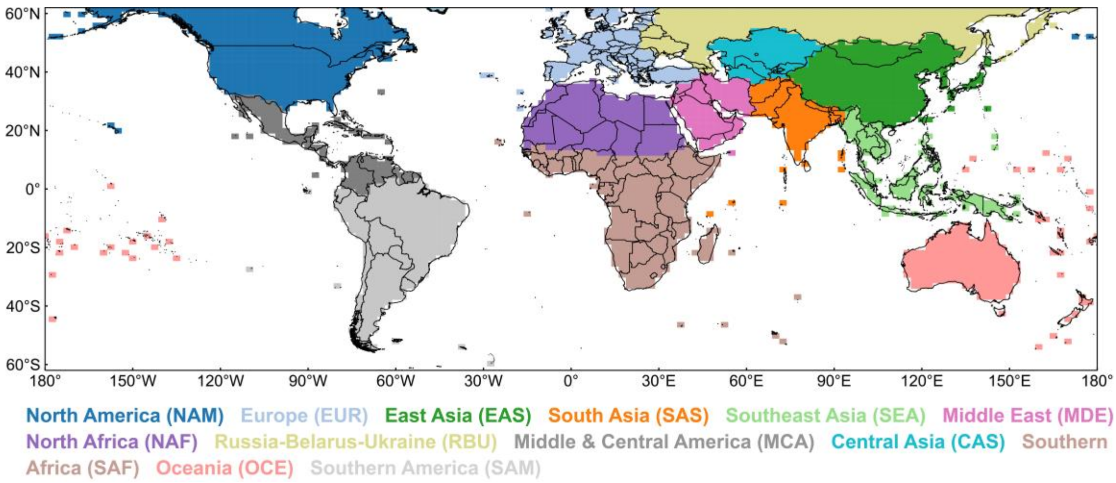

Figure S2. NO_x-tagged domain of the CAM4-chem simulation.

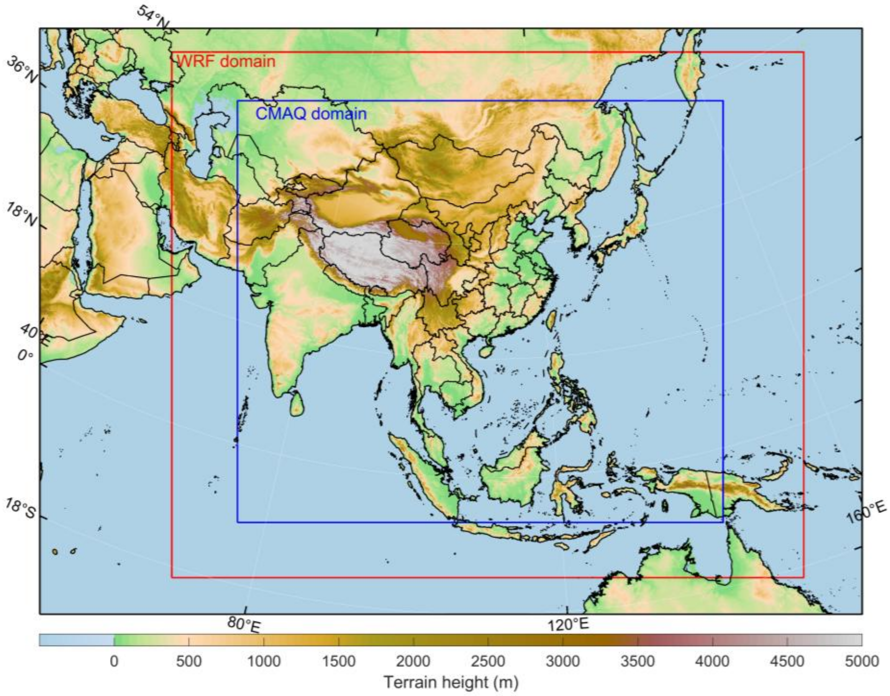

Figure S3. Domain of the WRF-CMAQ simulation.

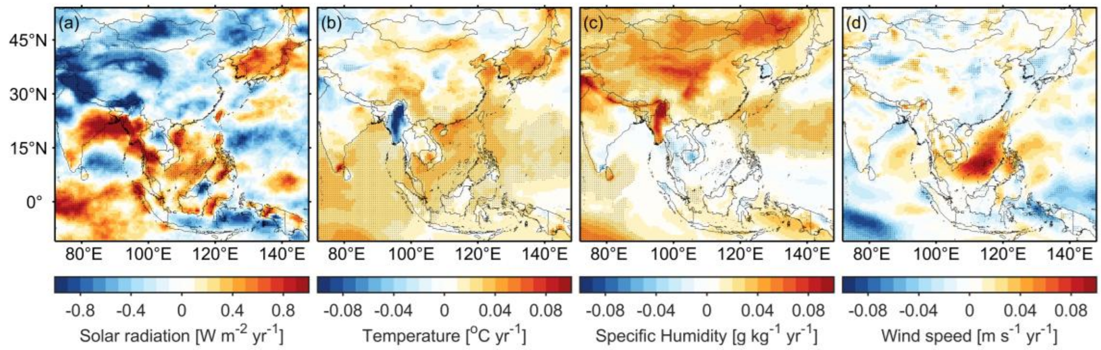

Figure S4. Spatial distributions of trends in meteorological variables over East and Southeast Asia, 1995-2019. Panels (a) to (d) displays trends in surface downward solar radiation, temperature at 2m height, specific humidity at 2m height and wind speed at 10m height, respectively. Meteorological parameters are derived from the MERRA2 re-analysis dataset. Black dots denoted linear trends with a p-value < 0.05.

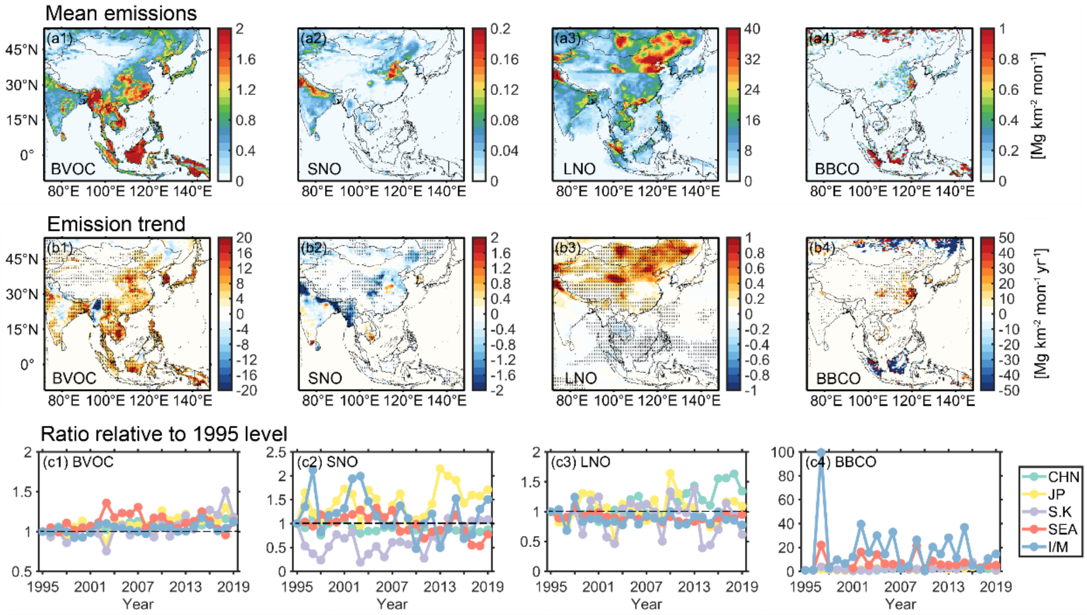

Figure S5. Same as Figure 2, but for BVOC, soil NO_x, and lightning NO emissions. Emissions are estimated from parameterization schemes implemented in the GEOS-Chem model, except for biomass burning emissions which are derived from the BB4CMIP6 and GFED inventory.

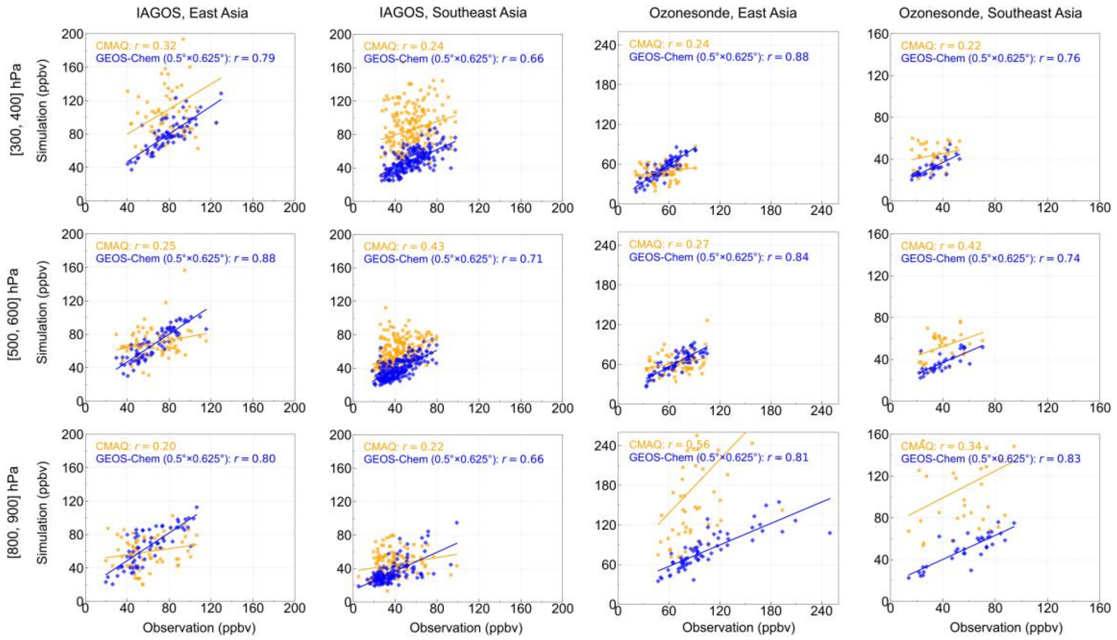

Figure S6. Evaluation of GEOS-Chem and WRF-CMAQ simulated summertime tropospheric ozone distributions over IAGOS regions and at ozonesonde sites. The comparisons are separated for the upper, middle, and lower troposphere. Correlation coefficients between the observed and simulated values are shown inset. Data descriptions are provided in the caption of Figure 3.

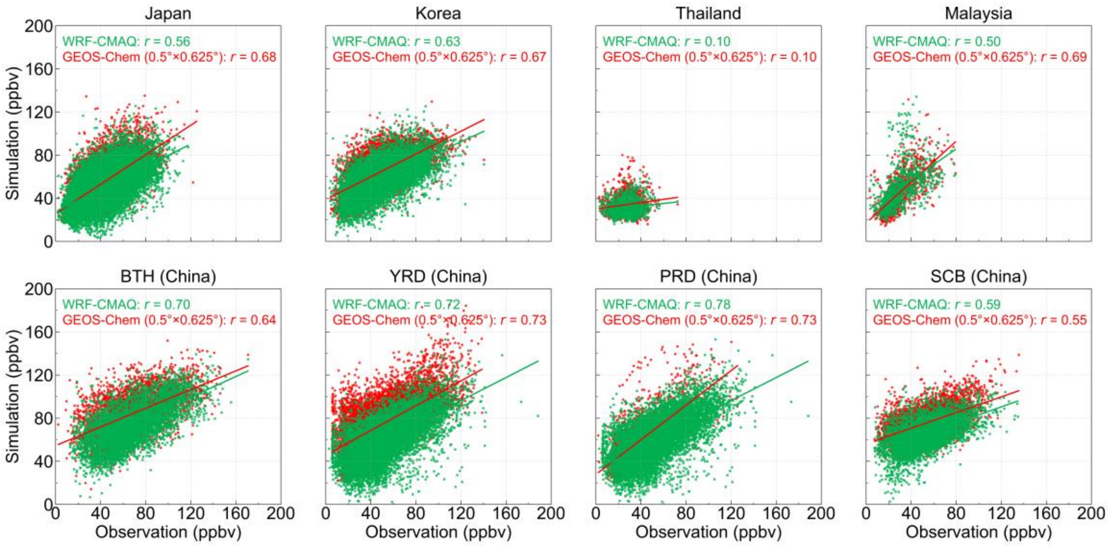

Figure S7. Evaluation of GEOS-Chem and WRF-CMAQ model simulated summertime surface MDA8 ozone concentrations over ESEA. Correlation coefficients between the observed and simulated values are shown inset. Same as Figure 4 but illustrated in scatter plots. CAM-Chem results are not shown as the spatial resolution is too coarse to resolve the ozone deviation at different sites.

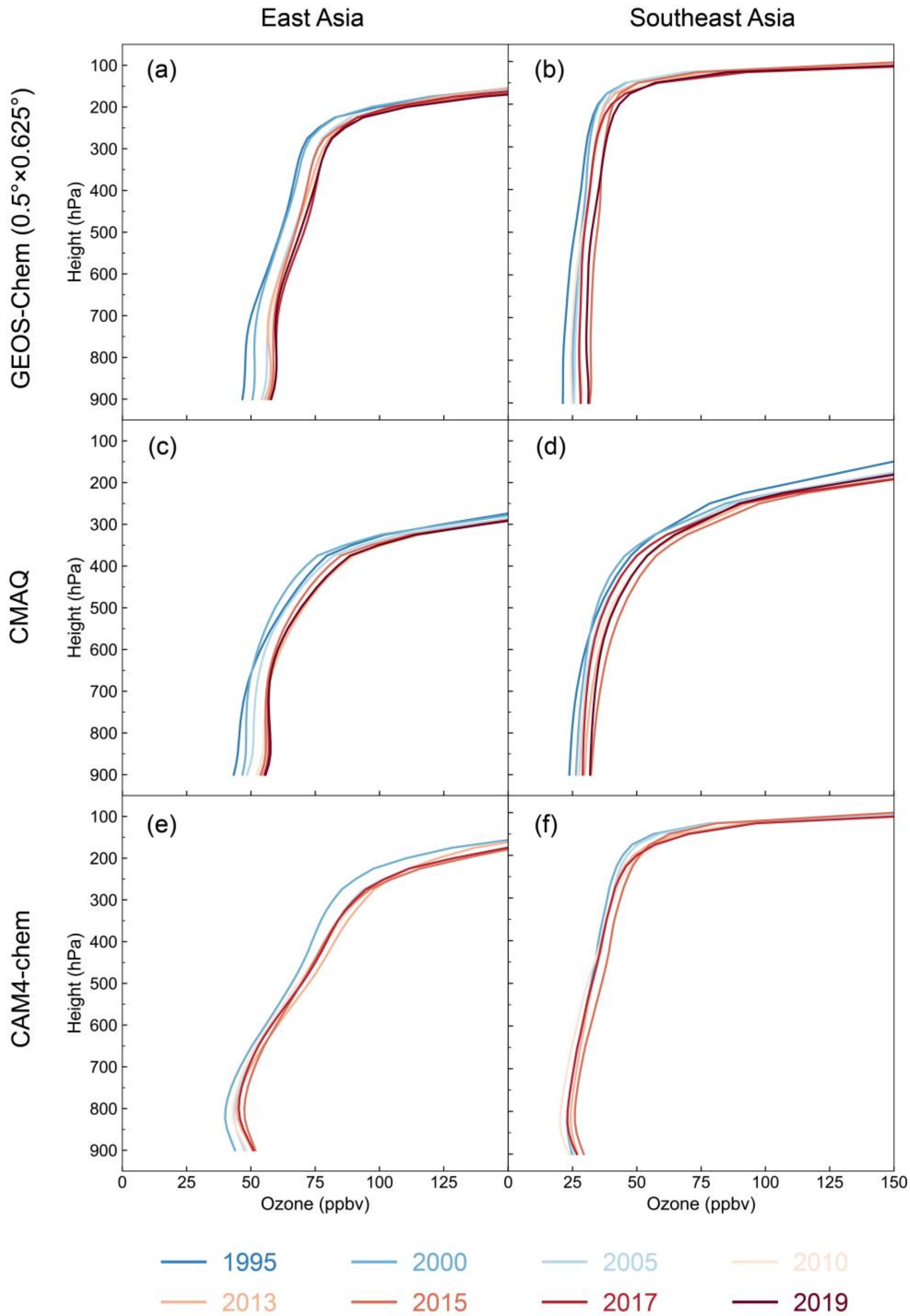

Figure S8. Comparison of GEOS-Chem, CMAQ, and CESM vertical ozone profiles averaged over East Asia and Southeast Asia in June, July, August in 1995-2019.

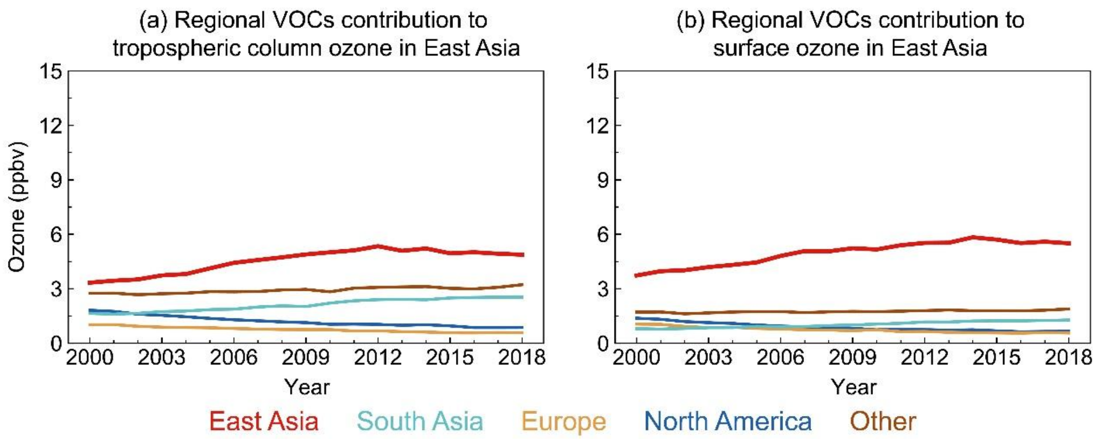

Figure S9. Same as Figure 10 but for RC-tagged results. Results for Southeast Asia is not available, because Southeast Asia is categorized as “Other” in RC-tagged simulation.

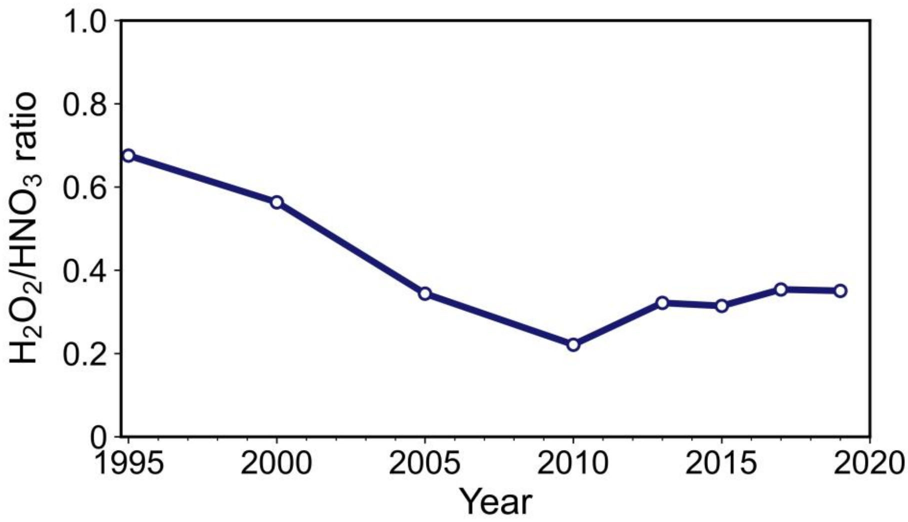

Figure S10. H_2O_2/HNO_3 time series in the North China Plain city cluster, China.

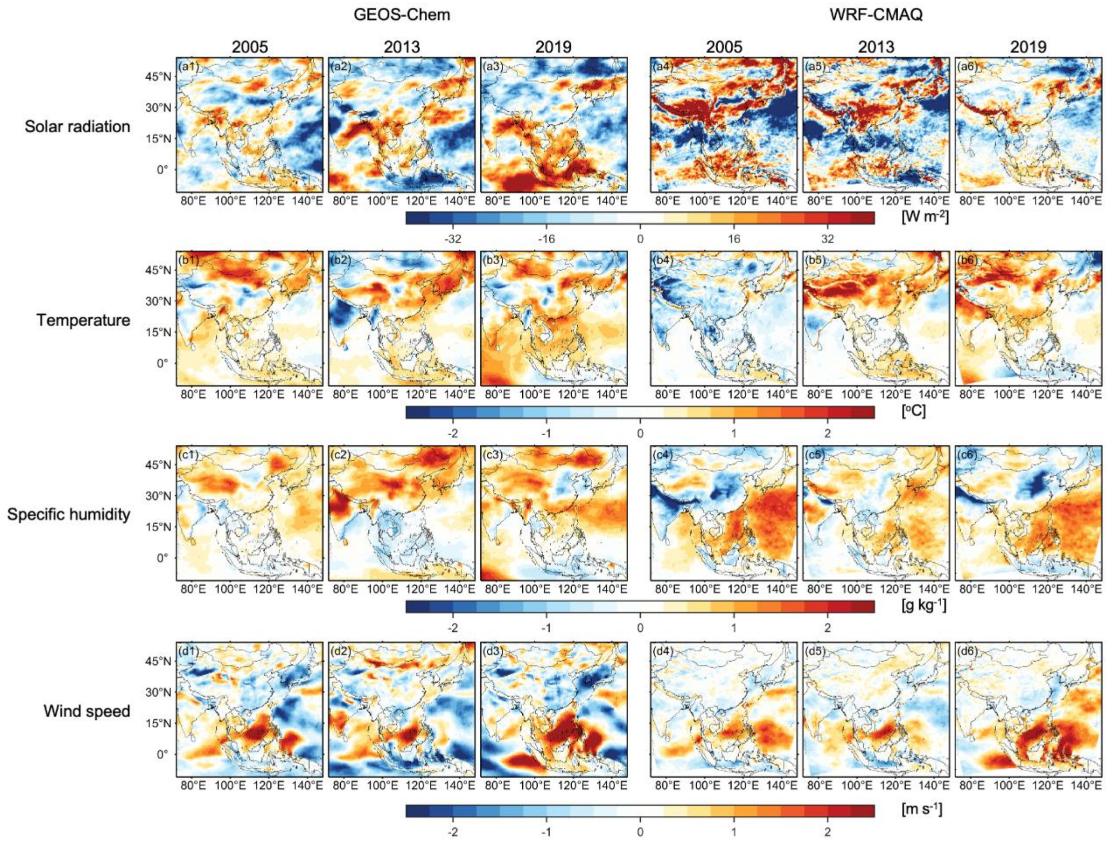

Figure S11. Differences in meteorological factors between the corresponding year and 1995 from the MERRA2 reanalysis data used to drive the GEOS-Chem model and the WRF model output used to drive the WRF-CMAQ model.

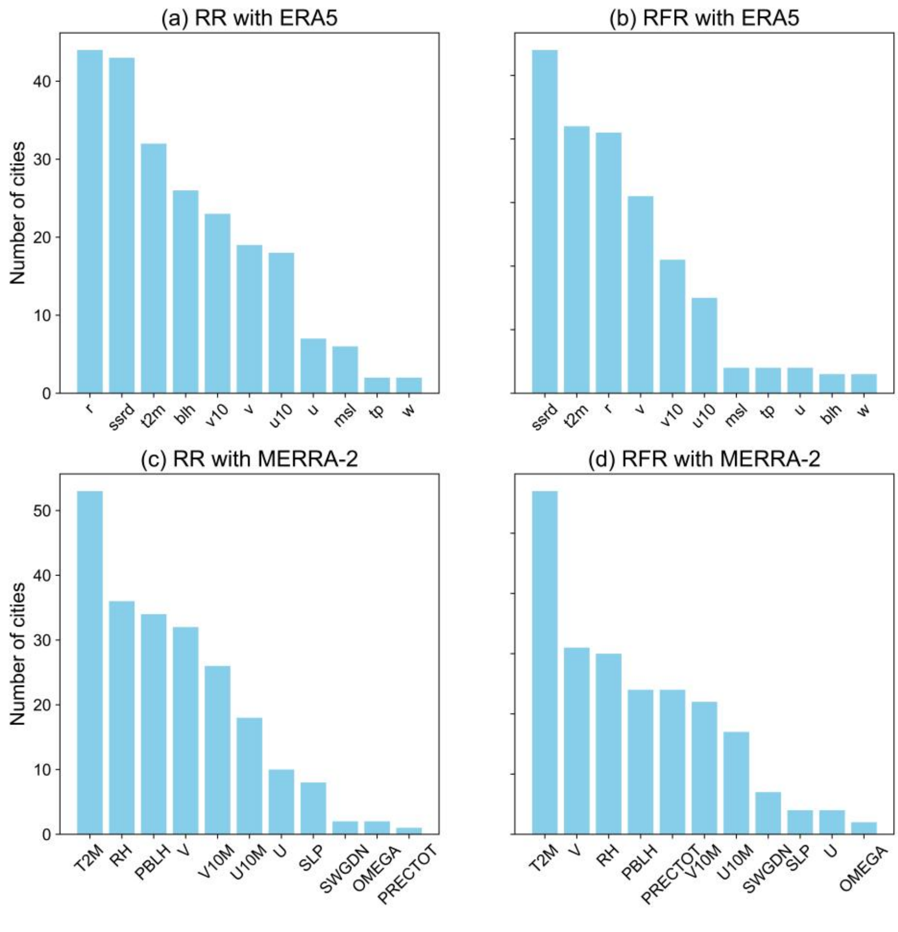

Figure S12. Number of cities with the meteorological parameters included as top-three most powerful predictors in the RR or RFR models.

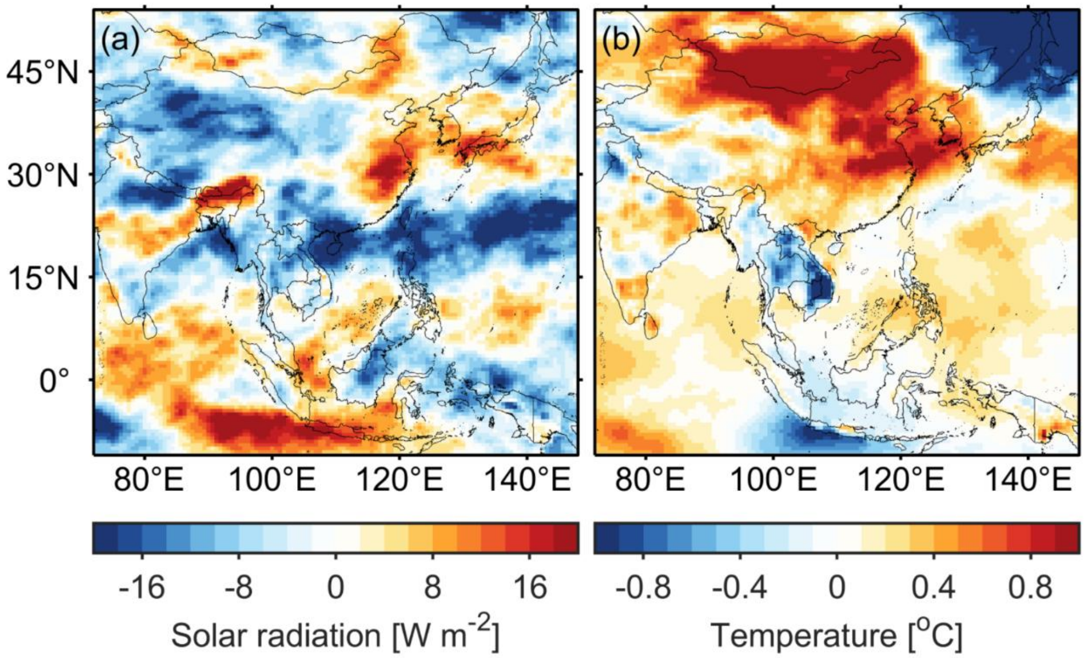

Figure S13. Difference in meteorological parameters in 2017-2019 and 2013-2015.